Light in Power: A General and Parameter-free Algorithm for Caustic Design

Quentin Mérigot, Jocelyn Meyron, Boris Thibert

LIGHT IN POWER: A GENERAL AND PARAMETER-FREE ALGORITHM FOR CAUSTIC DESIGN

QUENTIN MÉRIGOT, JOCELYN MEYRON, AND BORIS THIBERT

Abstract. We present in this paper a generic and parameter-free algorithm to efficiently build a wide variety of optical components, such as mirrors or lenses, that satisfy some light energy constraints. In all of our problems, one is given a collimated or point light source and a desired illumination after reflection or refraction and the goal is to design the geometry of a mirror or lens which transports exactly the light emitted by the source onto the target. We first propose a general framework and show that eight different optical component design problems amount to solving a *Light Energy Conservation* equation that involves the computation of *Visibility diagrams*. We show that these diagrams all have the same structure and can be obtained by intersecting a 3D Power Diagram with a planar or spherical domain. This allows us to propose an efficient and fully generic algorithm capable to solve the eight optical component design problems. Our solutions can satisfy design constraints such as convexity or concavity and are always graphs over the plane or the sphere. We show the effectiveness of our algorithm on numerous simulated examples.

1. Introduction

The field of non-imaging optics deals with the design of optical components whose goal is to transfer the radiation emitted by a light source onto a prescribed target. This question is at the heart of many applications where one wants to optimize the use of light energy by decreasing light loss or light pollution. Such problems appear in the design of car beams, public lighting, solar ovens and hydroponic agriculture. This problem has also been considered under the name of *caustic design*, with applications in architecture and interior decoration [9].

In this paper, we consider the problem of designing a wide variety of mirrors and lenses that satisfies different kinds of light energy constraints. To be a little bit more specific, in each problem that we consider, one is given a light source and a desired illumination after reflection or refraction which is called the target, and the goal is to design the geometry of a mirror or lens which transports exactly the light emitted by the source onto the target. Note that the design of these optical components can be regarded as an *inverse problem*, where the *direct problem* would be the simulation of the target illumination from the description of the light source and the geometry of the mirror or lens.

In practice, the mirror or lens needs to satisfy aesthetic and pragmatic design constraints. In many situations, such as for the construction of car lights, physical moulds are built by milling and the mirror or lens is built on this mould. Sometimes the optical component itself is directly milled. This imposes some constraints that can be achieved by imposing convexity or smoothness conditions. The convexity constraint is classical since it allows in particular to mill the component. Similarly, the concavity constraint allows to mill its mould. Remark also that when a mirror

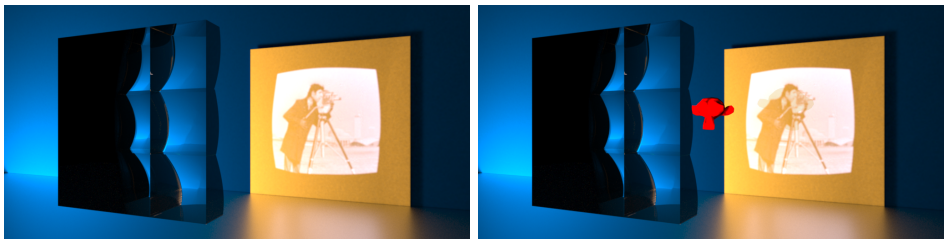

FIGURE 1. Our algorithm can be used to design mirrors and lenses that reflect or refract collimated or point light sources onto a prescribed distribution of light such as a greyscale image. *From left to right:* a lens composed of nine pillows that refracts a collimated light source; the same lens with an obstacle in red.

surface is convex, its chemical treatment is easier. Indeed, after construction, some liquid aluminum is deposited for the reflection. This liquid tends to concentrate where the surface contains small bumps or holes [6] and the convexity provides a way of avoiding these small bumps.

In this paper, we propose a generic algorithm capable of solving eight different caustic design problems, see Figures 1 and 2. Our approach is based on the fact that all of these problems are related to optimal transport and can be recast as solving a generalized Monge-Ampère equation. The algorithm is fully generic in the sense that it can deal with any of the eight caustic-design problems just by changing a formula, and can handle virtually any collimated or point light source and target.

We combine several ideas: we recast all caustic-design problems as a non-linear system of equations involving the notion of *Visibility cells*; we show that these Visibility cells have the same structure in all the cases, as they can be obtained by intersecting a 3D Power diagram with a planar or spherical domain; we solve this system using a damped Newton algorithm known to have a quadratic local convergence rate for optimal transport problems [14] or for Monge-Ampère equations in the plane [17].

To summarize, our contributions are the following:

- We propose a general framework for eight different optical component modeling problems (actually, we have four non-imaging problems; for each problem, we provide two solutions that have different properties, such as convexity or concavity). First, we show that in the eight cases, the problem amounts to solving the same non-linear equation that we call *Light Energy Conservation* (LEC) equation. This equation involves integrals over Visibility cells. Second, we show that these Visibility cells can be obtained in the eight cases by computing the intersection of a 3D Power diagram with a planar of spherical domain.
- We propose a generic algorithm capable to solve the eight different problems: we solve the (LEC) equation by a damped Newton algorithm. At each Newton step and in all of the eight cases, we evaluate a function that

amounts to computing integrals over the intersection of a 3D Power Diagram with a triangulation. The previous algorithms only deal with one case.
- Our algorithm is parameter-free: for each design problem, we obviously have a specific formula for a power diagram (involved in the computation of the Visibility cells) and a function (that parametrizes the lens or mirror surface), but no parameter.
- In all of the four non-imaging problems, we provide solutions that satisfy design constraints: in each case, we can provide a concave optical component. Furthermore, our solutions are always continuous graphs over either the plane or the sphere and are manifold and watertight.

2. Related work

The field of non-imaging optics has been extensively studied the last thirty years. We give below an overview of the main approaches to tackle several of the problems of this field.

2.1. **Non convex energy minimization methods.** Many different methods to solve inverse problems arising in non-imaging optics rely on variational approaches. When the energies to be minimized are not convex, this can be handled by different kind of iterative methods. A survey on inverse surface design from light transport behaviour can be found in [19].

One class of methods deals with stochastic optimization. In [9], the optical component (mirror or lens) is represented as a $\mathcal{C}^2$ B-spline triangle mesh and a stochastic optimization is used to adjust the heights of the vertices so as to minimize a light energy constraint. Note that this approach is very costly, since a forward simulation needs to be done at every step and the number of steps is very high in practice. Furthermore, using this method, lots of artifacts in the final caustic images are present.

Stochastic optimization has also been used in [18] to design reflective or refractive caustics for collimated light sources. At the center of the method is the Expectation Minimization algorithm initialized with a Capacity Constrained Voronoi Tessellation (CCVT) using a variant of the Lloyd's algorithm. The source is a uniform directional light and is modeled using an array of curved microfacets. The target is represented with a mixture of Gaussian kernel functions. This method cannot accurately handle low intensity regions and artefacts due to the discretization are present. Microfacets were also used in [24] to represent the mirror. Due to the sampling procedure, this method cannot correctly handle smooth regions and does not scale well with the size of the target.

The approaches of [13, 26, 22] have in common that they first compute some kind of relationship between the incident rays and their position on the target screen and then use an iterative method to compute the shape of the refractive surface. The method of [26] uses a continuous parametrization and thus cannot correctly handle totally black and high-contrast regions (boundaries between very dark and very bright areas).

The method proposed in [25] uses sticks to represent the refractive surface. This allows to reduce production cost, to be more entertaining for the user since a single set of sticks can produce different caustic patterns. The main problem with

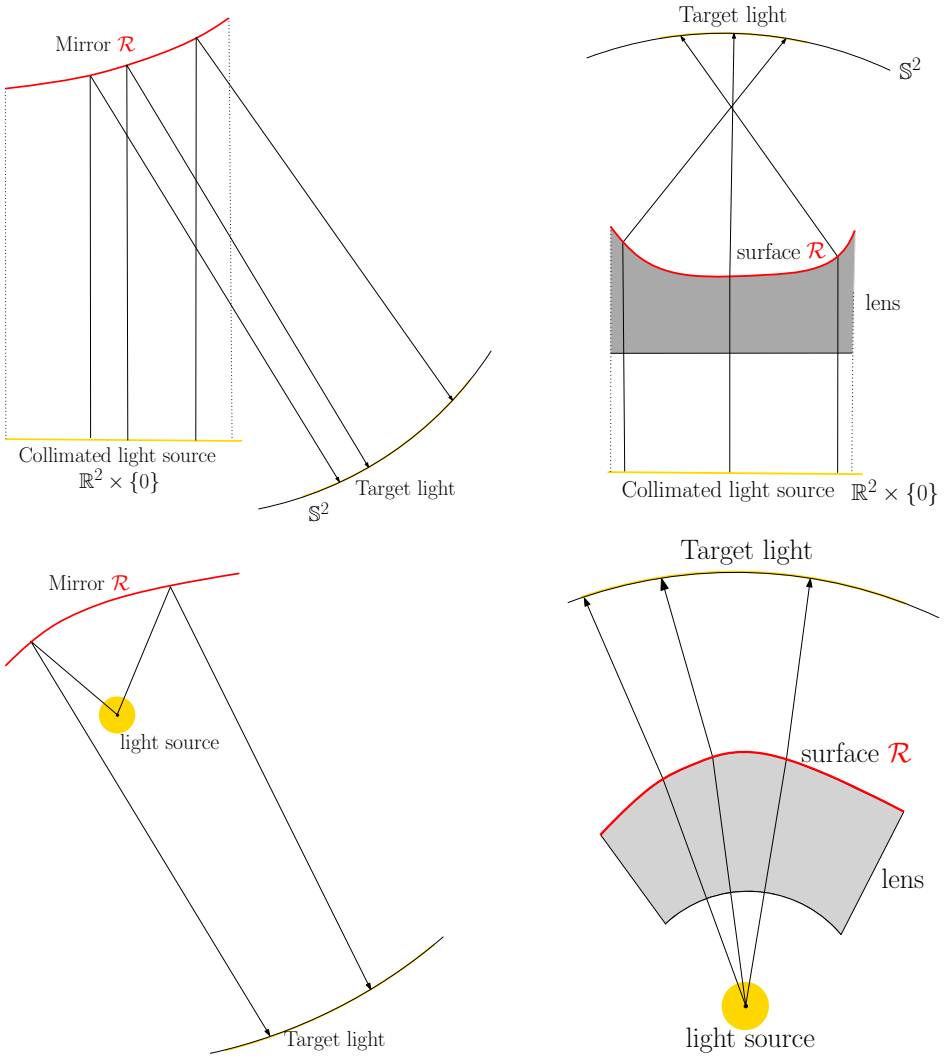

FIGURE 2. **Four inverse problems arising in non-imaging optics.** In each case, the goal is to build the surface $\mathcal{R}$ of a mirror or a lens. Remark that for each problem, we provide two solutions (for instance, we can have convex and concave surfaces when the light source is collimated). *Top/Bottom:* Collimated light sources/Point light sources. *Left/Right:* Mirror/Lens design problems.

this approach is the computational complexity since they need to solve a NP-hard assignment problem.

The problem of designing lenses associated to collimated light sources has also been considered in [22]. They propose a method to build lenses that can refract complicated and highly contrasted targets. They first use optimal transport on the

target space to compute a mapping between the refracted rays of an initial lens and the desired normals, then perform a post-processing step to build a surface whose normals are close to the desired ones.

2.2. **Monge-Ampère equations.** When the source and target lights are modeled by continuous functions, the problem amounts to solving a generalized Monge-Ampère equation, either in the plane for collimated light sources, or on the sphere for point light sources. These partial differential equations are highly non-linear. The existence and regularity of their solutions, namely of the mirror or lens surfaces, have been extensively studied. When the light source is punctual, this problem has been studied for mirrors [4, 5] and lenses [11] and when the light source is collimated we have the usual Monge-Ampère equation in the plane [12].

2.3. **Optimal transport based methods in non-imaging optics.** In fact, the Monge-Ampère equations corresponding to the non-imaging problems considered in this paper can be recast as optimal transport problems. This was first observed by [23] and [10] for the mirror problem with a point light source. Many algorithms related to optimal transport have been developed to address non-imaging problems. For example, a wide-stencil approach has been used to numerically solve a mirror design problem with a collimated light source [20]. Several methods have also been proposed when the light source is continuous and the target light is discrete: a variant of the Oliker-Prussner algorithm has been developed when the light source is punctual for the mirror problem [3] or the lens problem [11], but their $\mathrm{O}(N^4)$ complexity does not allow large discretizations. For the point light source mirror problem, a quasi-Newton method was proposed in [7] and the target light could have up to 15,000 diracs. Note also that the method developed in [16] or [8] to compute optimal transport for the quadratic cost in 2D could be applied to the non-imaging problems involving a collimated light source (see the next section for the details).

Note that the approach of [22] to build a lens also uses optimal transport. However, the optimal transport step is a heuristic for normal estimation and does not provide directly a solution to the non-imaging problem. A post-processing step is then performed by minimizing an energy composed of five weighted terms. In our approach, we directly solve eight optical component design problems, including the design of lenses for collimated light sources. Our approach is parameter-free and no post-processing is needed since the optimal transport formulation directly provides a solution. Note that physical constructions of lenses have already been proposed in [22] and will not be considered here.

Acknowledgements. This work has been partially supported by the LabEx PERSYVAL-Lab (ANR-11-LABX-0025-01) funded by the French program Investissement davenir and by ANR-16-CE40-0014 - MAGA - Monge Ampère et Géométrie Algorithmique.

3. Light Energy Conservation

We present in this section several mirror and lens design problems arising in non-imaging optics. In all the problems, one is given a light source (emitted by either a plane or a point) and a desired illumination "at infinity" after reflection or refraction, which is called the target, and the goal is to design the geometry of a mirror or lens which transports the energy emitted by the source onto the

target. Even though the problems we consider are quite different from one another, they share a common structure that corresponds to a so-called generalized Monge-Ampère equation.

Roughly speaking, given a light source modeled by an illumination density ρ and a target light modeled by a function σ, the problem amounts to finding a reflection (or refraction) map F that preserves the light energy, namely that satisfies the following *Light Energy Conservation* equation

$$(LEC_{cont}) \qquad \sigma(F(x))|\det(DF(x))| = \rho(x).$$

We are going to show that one can rewrite this conservation equation in many different problems when the target is supported on a finite point set.

3.1. **Mirror design.**

3.1.1. *Convex mirror for a collimated light source.* In the first design problem we consider, the light source is collimated, meaning that all rays are parallel, and can be encoded by a light intensity function ρ over a 2D domain. The desired target illumination is "at infinity", and is described by a set of intensity values $\sigma = (\sigma_i)_{1\leqslant i\leqslant N}$ supported on the finite set of directions $Y = \{y_1, \cdots, y_N\}$ included in the unit sphere $\mathbb{S}^2$. The problem is to find the surface $\mathcal{R}$ of a mirror that sends the source intensity ρ to the target intensity σ, see Figures 2 and 3. This problem corresponds to a Monge-Ampère equation in the 2D plane that is also known to be an optimal transport problem for the quadratic cost [20].

Since the number of reflected directions Y is finite, the mirror surface $\mathcal{R}$ is supported by a finite number of planes, as illustrated in Figure 3. We define $\mathcal{R}$ as the graph of a convex function of the form $x \mapsto \max_i \langle x|p_i\rangle - \psi_i$, where $\langle\cdot|\cdot\rangle$ denotes the usual dot product in $\mathbb{R}^3$ and for every $i \in \{1, \cdots, N\}$, p_i is the slope of the plane that reflects according to Snell's law the vertical ray $(0, 0, 1)$ to the direction y_i (see Section 5 for the full expression) and ψ_i is a real number that encodes the elevation of the supporting plane with slope p_i. We denote by $\psi := (\psi_i)_{1\leqslant i\leqslant N}$ the set of elevations. We define the Visibility cell $\mathrm{V}_i(\psi)$ of y_i as the set of points $x \in \mathbb{R}^2 \times \{0\}$ that are reflected to the direction y_i. By construction, the vertical ray emanating from the point $x \in \mathbb{R}^2 \times \{0\}$ touches the mirror surface $\mathcal{R}$ at an altitude $\langle x|p_i\rangle - \psi_i$ for a given i and is reflected to the direction y_i. Hence the Visibility cell is given by

$$\mathrm{V}_i(\psi) = \{x \in \mathbb{R}^2 \times \{0\} \mid \ -\langle x|p_i\rangle + \psi_i \leqslant -\langle x|p_j\rangle + \psi_j \ \forall j\}.$$

Remark that the intensity of light reflected to the direction y_i equals $\int_{\mathrm{V}_i(\psi)} \rho(x)\mathrm{d}x$. Hence the *Collimated Source Mirror problem* (CS/Mirror) amounts to finding weights $(\psi_i)_{1\leqslant i\leqslant N}$ such that

$$\text{(LEC)} \qquad \forall i \in \{1, \cdots, n\} \quad \int_{\mathrm{V}_i(\psi)} \rho(x)\mathrm{d}x = \sigma_i.$$

Remark that this *Light Energy Conservation* (LEC) equation is a discrete version of Equation (LEC_{cont}) since σ is finitely supported. By construction, a solution to the (LEC) equation provides a parameterization $\mathcal{R}_\psi$ of a convex mirror that sends the collimated light source ρ to the discrete target σ:

$$\mathcal{R}_\psi : \ x \in \mathbb{R}^2 \ \mapsto \ (x, \max_i \langle x|p_i\rangle - \psi_i),$$

where $\mathbb{R}^2 \times \{0\}$ and $\mathbb{R}^2$ are identified. Notice that since the mirror is a graph over $\mathbb{R}^2 \times \{0\}$, the vectors y_i cannot be upward vertical. In practice, we suppose that the directions y_i are downward, *i.e.* that $y_i \in \mathbb{S}^2_- := \{x \in \mathbb{S}^2,\ \langle x|e_z\rangle \leqslant 0\}$. Furthermore, we localize the position of the mirror by considering it only above the support $X_\rho := \{x \in \mathbb{R}^2 \times \{0\}, \rho(x) \neq 0\}$ of ρ.

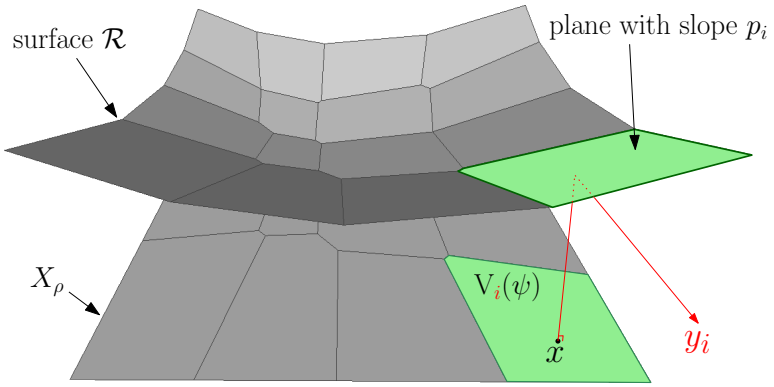

FIGURE 3. **Convex Mirror for a collimated light source** (when $N = 16$). The mirror surface $\mathcal{R}$ is the graph of a convex piecewise affine function. The support X_ρ of ρ is decomposed into Visibility cells $(V_i(\psi))_{1\leqslant i\leqslant N}$. Every vertical ray above a point $x \in X_\rho$ belongs to a cell $V_i(\psi)$, touches a plane of slope p_i and is reflected to the direction y_i.

3.1.2. *Concave mirror.* Note that with our approach, we can also build concave mirrors, by considering a parameterization with a concave function of the form $x \mapsto \min_i \langle x|p_i\rangle + \psi_i$. This amounts to replacing p_i by its opposite in the Visibility cell, namely to have

$$\mathrm{V}_i(\psi) = \{x \in \mathbb{R}^2 \times \{0\} \mid\ \langle x|p_i\rangle + \psi_i \leqslant \langle x|p_j\rangle + \psi_j\ \forall j\}.$$

In that case, a solution to (LEC) provides a parametrization of a concave mirror $\mathcal{R}_\psi(x) = (x, \min_i \langle x|p_i\rangle + \psi_i)$ that sends the collimated light source ρ to the discrete target σ.

3.1.3. *Concave mirror for a point source.* In the second mirror design problem, all the rays are emitted from a single point in space, located at the origin, and the light source is described by an intensity function on the unit sphere $\mathbb{S}^2$. The target is as in the previous case "at infinity", and is described by a set of intensity values $\sigma = (\sigma_i)_{1\leqslant i\leqslant N}$ supported on the finite set of directions $Y = \{y_1, \cdots, y_N\} \subset \mathbb{S}^2$. The problem we consider is to find the surface $\mathcal{R}$ of a mirror that sends the light intensity ρ to the light intensity σ, see the bottom left diagram in Figure 2. This problem corresponds to a Monge-Ampère equation on the sphere [4] and can be recast as an optimal transport problem on the sphere [23] for the cost function $c(x, y) = -\ln(1 - \langle x|y\rangle)$.

Following [4], we build a concave surface $\mathcal{R}$ that is composed of pieces of confocal paraboloids. More precisely, we denote by $P(y_i, \psi_i)$ the solid (i.e filled) paraboloid whose focal point is at the origin and with focal distance ψ_i and define the surface $\mathcal{R}$ as the boundary of the intersection of the solid paraboloids, namely $\mathcal{R} = \partial\left(\cap_i P(y_i, \psi_i)\right)$. We define the Visibility cell $\mathrm{V}_i(\psi)$ as the set of rays $x \in \mathbb{S}^2$ emanating from the light source that are reflected to the direction y_i. Using the fact that each paraboloid $\partial P(y_i, \psi_i)$ is parameterized over the sphere by $x \mapsto \psi_i x/(1 - \langle x|y_i\rangle)$, one has [4]

$$\mathrm{V}_i(\psi) = \left\{ x \in \mathbb{S}^2,\ \frac{\psi_i}{1 - \langle x|y_i\rangle} \leqslant \frac{\psi_j}{1 - \langle x|y_j\rangle}\ \forall j \right\}.$$

The *Point Source Mirror problem* (PS/Mirror) then amounts to finding weights $(\psi_i)_{1\leqslant i\leqslant N}$ that satisfy the Light Energy Conservation equation (LEC). Remark that, once Equation (LEC) is solved, the mirror surface is then given by the parameterization

$$\mathcal{R}_\psi :\ x \in \mathbb{S}^2\ \mapsto\ \min_i \frac{\psi_i}{1 - \langle x|y_i\rangle}\ x.$$

In practice, we choose the set of directions y_i to belong to $\mathbb{S}^2_-$ and the mirror to be parameterized over the support $X_\rho := \{x \in \mathbb{S}^2, \rho(x) \neq 0\}$ of ρ which is chosen to be included in $\mathbb{S}^2_+ := \{x \in \mathbb{S}^2,\ \langle x|e_z\rangle \geqslant 0\}$.

Remark. One can also define the mirror surface as the boundary of the union (instead of the intersection) of a family of solid paraboloids. In that case, the Visibility cells are given by

$$\mathrm{V}_i(\psi) = \left\{ x \in \mathbb{S}^2,\ \frac{\psi_i}{1 - \langle x|y_i\rangle} \geqslant \frac{\psi_j}{1 - \langle x|y_j\rangle}\ \forall j \right\}$$

and a solution to Equation (LEC) provides a parameterization $\mathcal{R}_\psi(x) = x \max_i \psi_i/(1 - \langle x|y_i\rangle)$ of the mirror surface.

3.2. **Lens design.** In this section, the goal is to design lenses that refracts a given light source intensity to a desired one. Similarly to mirror design, we consider collimated and point light sources. We denote by n_1 the refractive index of the lens, by n_2 the ambient space refractive index and by $\kappa = n_1/n_2$ the ratio of the two indices.

3.2.1. *Concave lens for a collimated light source.* We consider here a collimated light source encoded by a function ρ in the plane and a target illumination supported on a finite set $Y = \{y_1, \cdots, y_N\} \subset \mathbb{S}^2$ encoded by $\sigma = (\sigma_i)_{1\leqslant i\leqslant N}$. The goal is to find the surface of a lens that sends ρ to σ, see the top right diagram in Figure 2.

By a simple change of variable, we show that this problem is equivalent to (CS/Mirror). More precisely, for every $y_i \in Y$, we now define p_i to be the slope of a plane that refracts the vertical ray $(0, 0, 1)$ to the direction y_i (see Section 5 for a detailed expression). We define $\mathcal{R}$ as the graph of a convex function of the form $x \mapsto \max_i \langle x|p_i\rangle - \psi_i$, where $\psi = (\psi_i)_{1\leqslant i\leqslant N}$ is the set of elevations. We define the Visibility cell $\mathrm{V}_i(\psi)$ to be the set of points $x \in \mathbb{R}^2 \times \{0\}$ that are refracted to the direction y_i:

$$\mathrm{V}_i(\psi) = \{x \in \mathbb{R}^2 \times \{0\} \mid \forall j,\ -\langle x|p_i\rangle + \psi_i \leqslant -\langle x|p_j\rangle + \psi_j\}.$$

The *Collimated Source Lens problem* (CS/Lens) then amounts to finding weights $(\psi_i)_{1\leqslant i\leqslant N}$ that satisfy (LEC). In that case the lens surface is parameterized by

$$\mathcal{R}_\psi : \ x \in \mathbb{R}^2 \ \mapsto \ (x, \max_i \langle x|p_i\rangle - \psi_i).$$

In practice, we choose the directions y_i in $\mathbb{S}^2_+$ and the mirror to be parameterized over the support X_ρ of ρ.

3.2.2. *Convex lens.* Remark that we can also build convex lenses by considering parameterizations with concave functions of the form $x \mapsto \min_i \langle x|p_i\rangle + \psi_i$. This amounts to replacing p_i by its opposite in the Visibility cell. A solution to (LEC) then provides a parametrization of a convex lens $\mathcal{R}_\psi(x) = (x, \min_i \langle x|p_i\rangle + \psi_i)$ that sends the collimated light source ρ to the discrete target σ.

3.2.3. *Convex lens for a point source.* We now consider the same problem, except that we replace the collimated light source by a point source one. It has been shown in [11] that the lens can be made by pieces of ellipsoids of constant eccentricities κ, where κ is the ratio of the indices of refraction. More precisely, if we denote by $E(y_i, \psi_i)$ the solid ellipsoid with focal points the origin and y_i, then $\mathcal{R}$ is the boundary $\partial(\cap_i E(y_i, \psi_i))$ of the intersection of the solid ellipsoids. Using the fact that each ellipsoid $\partial E(y_i, \psi_i)$ can be parameterized over the sphere by $x \mapsto \psi_i x/(1-\kappa\langle x|y_i\rangle)$, the Visibility cell of y_i is given by [11]

$$\mathrm{V}_i(\psi) = \left\{ x \in \mathbb{S}^2, \ \frac{\psi_i}{1-\kappa\langle x|y_i\rangle} \leqslant \frac{\psi_j}{1-\kappa\langle x|y_j\rangle} \ \forall j \right\}.$$

The *Point Source Lens problem* (PS/Lens) then amounts to finding weights $(\psi_i)_{1\leqslant i\leqslant N}$ that satisfy (LEC). Remark that the lens surface is parameterized by

$$\mathcal{R}_\psi : \ x \in \mathbb{S}^2 \ \mapsto \ \min_i \frac{\psi_i}{1-\kappa\langle x|y_i\rangle} \ x.$$

In practice, we choose the set of directions y_i to belong to $\mathbb{S}^2_+$ and the lens to be parameterized over the support $X_\rho \subset \mathbb{S}^2_+$ of ρ.

Remark. One can also choose to define the lens surface as the boundary of the union (instead of the intersection) of a family of solid ellipsoids. In that case, the Visibility cells are given by

$$\mathrm{V}_i(\psi) = \left\{ x \in \mathbb{S}^2, \ \frac{\psi_i}{1-\kappa\langle x|y_i\rangle} \geqslant \frac{\psi_j}{1-\kappa\langle x|y_j\rangle} \ \forall j \right\}$$

and a solution to Equation (LEC) provides a parameterization $\mathcal{R}_\psi(x) = x \max_i \psi_i/(1-\kappa\langle x|y_i\rangle)$ of the lens surface.

3.3. **General formulation.** We have presented four optical component design problems. For each problem, we provide two solutions (that correspond to convex and concave ones for collimated light sources). We underline in this section that all these problems amount to finding the zero of a function that involves a decomposition of the plane or the unit sphere into a finite number of cells.

Let X be a domain of either the plane $\mathbb{R}^2 \times \{0\}$ or the unit sphere $\mathbb{S}^2$, $\rho : X \to \mathbb{R}$ a density measure and $Y = \{y_1, \cdots, y_N\} \subset \mathbb{S}^2$ be a set of N points. We define the function $G : \mathbb{R}^N \to \mathbb{R}^N$ by

$$G_i(\psi) = \int_{\mathrm{V}_i(\psi)} \rho(x)\mathrm{d}x$$

where $G(\psi) = (G_i(\psi))_{1 \leqslant i \leqslant N}$ and $\mathrm{V}_i(\psi) \subset X$ is the Visibility cell of y_i that depends on the non-imaging problem. The common problem to all the one mentioned above is to find a set of weights $\psi = (\psi_i)_{1 \leqslant i \leqslant N}$ such that

$$\forall i \in \{1, \cdots, N\} \quad G_i(\psi) = \sigma_i. \tag{LEC'}$$

One may remark that the decomposition into Visibility cells $\mathrm{V}_i(\psi)$ forms almost everywhere a partition of X when ρ does not vanish.

Remark. Many other problems arising in non-imaging optics amount to solving Equation (LEC'). For example, the design of a lens that refracts a point light source to a desired near-field target can also be modeled by a Monge-Ampère equation that has the same structure [11]. In this case, the Visibility diagram correspond to the radial projection onto the sphere of pieces of confocal ellipsoids with non constant eccentricity and it is not associated to an optimal transport problem.

4. Visibility and Power cells

We saw in the previous section that several non-imaging problems have the same structure and amount to solving an equation of the form $G(\psi) = \sigma$, where $G : \mathbb{R}^N \to \mathbb{R}^N$ is a function and ψ is the unknown. However, in this formulation, the function G depends on the Visibility cells associated to each optical modeling problem.

We show in this section that the Visibility cells have always the same structure. This point is crucial and will allow us to build a generic algorithm in Section 5. More precisely, we show that in all the non-imaging problems of Section 3, the Visibility cells are of the form

$$V_i(\psi) = \mathrm{Pow}_i(\mathrm{P}) \cap X.$$

In this equation, X denotes either the plane $\mathbb{R}^2 \times \{0\}$ if the light source is collimated or the unit sphere $\mathbb{S}^2$ if the light source is punctual. The sets $\mathrm{Pow}_i(\mathrm{P})$ are the usual power cells of a weighted point cloud $\mathrm{P} = \{(p_i, \omega_i)\} \subset \mathbb{R}^3 \times \mathbb{R}$:

$$\mathrm{Pow}_i(\mathrm{P}) := \{x \in \mathbb{R}^3 \mid \forall j,\ \|x - p_i\|^2 + \omega_i \leqslant \|x - p_j\|^2 + \omega_j\}.$$

4.1. **Convex mirror for (CS/Mirror).** We first consider the convex mirror modeling problem when the light source is collimated. First recall that $p_i \in \mathbb{R}^2 \times \{0\}$ is the slope of the plane that reflects with the Snell's law the upward vertical ray $e_z := (0, 0, 1)$ to the direction y_i. A straightforward calculation shows that $p_i = \mathrm{p}_{\mathbb{R}^2}(y_i - e_z)/\langle y_i - e_z | e_z \rangle$, where $\mathrm{p}_{\mathbb{R}^2}$ denotes the orthogonal projection onto $\mathbb{R}^2 \times \{0\}$. Another simple calculation shows that the Visibility cell of y_i is given by $V_i(\psi) = \{x \in \mathbb{R}^2 \times \{0\}, \|x - p_i\|^2 + \omega_i \leqslant \|x - p_j\|^2 + \omega_j\ \forall j\}$, where $\omega_i = 2\psi_i - \|p_i\|^2$. We conclude that the Visibility cells of a convex mirror for (CS/Mirror) are given by $V_i(\psi) = \mathrm{Pow}_i(\mathrm{P}) \cap (\mathbb{R}^2 \times \{0\})$, where the weighted point cloud $\mathrm{P} = \{(p_i, \omega_i)\}$ is given by

$$p_i = \frac{\mathrm{p}_{\mathbb{R}^2}(y_i - e_z)}{\langle y_i - e_z | e_z \rangle} \quad \text{and} \quad \omega_i = 2\psi_i - \|p_i\|^2 .$$

Remark that if we want to build a concave mirror, one can simply replace p_i by its opposite, as explained in Section 3.

4.2. **Concave lens for (CS/Lens).** A similar calculation shows that the Visibility cells of a concave lens for (CS/Lens) are given by $V_i(\psi) = \mathrm{Pow}_i(\mathrm{P}) \cap (\mathbb{R}^2 \times \{0\})$, where the weighted point cloud $\mathrm{P} = \{(p_i, \omega_i)\}$ is given by

$$p_i = -\frac{\mathrm{p}_{\mathbb{R}^2}(y_i - \kappa e_z)}{\langle y_i - \kappa e_z | e_z \rangle} \quad \text{and} \quad \omega_i = 2\psi_i - \|p_i\|^2 .$$

Remark that if we want to build a convex lens, one can simply replace p_i by its opposite.

4.3. **Convex mirror for (PS/Mirror).** It was shown in [7] that when the mirror is the boundary of the intersection of solid paraboloids, the Visibility cells are obtained by intersecting a power diagram with the unit sphere. More precisely, one has $V_i(\psi) = \mathrm{Pow}_i(\mathrm{P}) \cap \mathbb{S}^2$, where the weighted point cloud $\mathrm{P} = \{(p_i, \omega_i)\}$ is given by

$$p_i = -\frac{y_i}{2\ln(\psi_i)} \text{ and } \omega_i = -\frac{1}{\ln(\psi_i)} - \frac{1}{4\ln(\psi_i)^2}.$$

If one wants to build the mirror as the boundary of the union of solid paraboloids, then the weighted point cloud $\mathrm{P} = \{(p_i, \omega_i)\}$ is given by $p_i = y_i/(2\ln(\psi_i)$ and $\omega_i = 1/\ln(\psi_i)) - 1/(4\ln(\psi_i)^2)$.

4.4. **Convex lens for (PS/Lens).** Its was shown in [11] that the Visibility cells are obtained in this case by projecting the intersection of confocal solid ellipsoids onto the sphere when $\kappa < 1$. It was also shown in [7] that an intersection of ellipsoids can be obtained by intersecting a power diagram with the unit sphere. Combining these results, one gets that $V_i(\psi) = \mathrm{Pow}_i(\mathrm{P}) \cap \mathbb{S}^2$, where the weighted point cloud $\mathrm{P} = \{(p_i, \omega_i)\}$ is given by

$$p_i = -\kappa\frac{y_i}{2\ln(\psi_i)} \text{ and } \omega_i = -\frac{1}{\ln(\psi_i)} - \frac{\kappa^2}{4\ln(\psi_i)^2}.$$

If we choose to define the lens surface as the boundary of the union of ellipsoids, then the weighted point cloud becomes $p_i = \kappa y_i/(2\ln(\psi_i))$ and $\omega_i = 1/\ln(\psi_i) - \kappa^2/(4\ln(\psi_i)^2)$.

5. A generic algorithm

We propose in this section a generic algorithm to efficiently build eight different kinds of optical design components (for each of the four non-imaging problems, we have two solutions).

5.1. **Overview of the algorithm.** For each optical design problem, given a light source intensity function, a target light intensity function and an error parameter, Algorithm 1 outputs a triangulation of a mirror or a lens that satisfies (LEC). Our algorithm combines several non-trivial ideas:

- **Damped Newton algorithm.** As previously seen, the main problem is to find the zero of a function. This is done with a damped Newton algorithm similar to recent algorithms that have been shown to have a quadratic local convergence rate for optimal transport problems [14] or for Monge-Ampère equations in the plane [17].

- **Non-empty Visibility cells.** We enforce all along the process the Visibility cells to be non empty, or more precisely to have $G_i(\psi) > 0$ for every i. Note that this condition is necessary: indeed, if a Visibility cell $V_i(\psi)$ is empty, then it remains empty for a small perturbation of ψ. This implies that the function G_i is locally constant, hence the i-th line of the matrix of $\mathrm{D}G(\psi)$ is vanishing, which implies that $G_i(\psi)$ remains equal to zero during the Newton algorithm.
- **Generic evaluation of G and Power diagrams.** In order to have a generic evaluation of G at $\psi \in \mathbb{R}^N$, we calculate the intersection of a 3D Power diagram with a triangulation T of the support X_ρ of ρ. This can be efficiently done for instance by using the algorithm developed in [15].
- **Generic evaluation of $\mathrm{D}G$ and Automatic differentiation.** We first calculate the vertices of the Visibility diagram in terms of the weights $\psi_1, \cdots, \psi_N$. Then, since the integrals depend on these vertices, we can use the *Automatic differentiation* technique [21] to compute automatically their derivatives with respect to the weights, hence we get $\mathrm{D}G$. In practice, one implements this technique by overloading the number type and the majority of the numerical operations.

ALGORITHM 1: Mirror / lens construction

Input: A light source intensity function ρ_{in}.
A target light intensity function σ_{in}.
A tolerance $\eta > 0$.
Output: A triangulation $\mathcal{R}_T$ of a mirror or lens $\mathcal{R}$.
Step 1: Initialization (Section 5.2)
$T, \rho \leftarrow$ `DISCRETIZATION_SOURCE`(ρ_{in})
$Y, \sigma \leftarrow$ `DISCRETIZATION_TARGET`(σ_{in})
$\psi^0 \leftarrow$ `INITIAL_WEIGHTS`(Y)
Step 2: Solve the (LEC') equation: $G(\psi) = \sigma$ (Section 5.3)
$\psi \leftarrow$ `DAMPED_NEWTON`$(T, \rho, Y, \sigma, \psi^0, \eta)$
Step 3: Construct a triangulation $\mathcal{R}_T$ of $\mathcal{R}$ (Section 5.4)
$\mathcal{R}_T \leftarrow$ `SURFACE_CONSTRUCTION`$(\psi, \mathcal{R}_\psi)$

5.2. **Initialization.**

5.2.1. *Discretization of light intensity functions.* Our framework allows to handle any kind of source or target light intensity functions. It can be for example any positive function on the plane or the sphere (depending on the problem) or a greyscale image. If the support of ρ is continuous, we discretize it by a triangulation T and consider a density $\rho : T \to \mathbb{R}^+$ affine on each triangle. We then normalize ρ by dividing it by the total integral $\int_T \rho(x)\mathrm{d}x$.

Similarly, the target light intensity function can also be discrete, such as an image on the unit sphere. If not, it can be discretized into a discrete measure of the form $\sigma = \sum_i \sigma_i \delta_{y_i}$ using, for instance, Lloyd's algorithm. It is also normalized by dividing with the discrete integral $\sum_i \sigma_i$.

Note that in order to handle black regions, we remove the directions y_i corresponding to black pixels (*i.e.* when $\sigma_i = 0$). This implies that no light will be sent towards black regions and avoids to have empty visibility cells.

5.2.2. *Choice of the initial family of weights ψ^0.* As mentioned at the beginning of Section 5.1, we need to ensure that at each iteration all the Visibility cells have non-empty interiors. In particular, we need to choose a set of initial weights $\psi^0 = (\psi_i^0)_{1 \leqslant i \leqslant N}$ such that the initial Visibility cells are not empty.

- For the collimated light sources cases (CS/Mirror) and (CS/Lens), we see that if we choose $\psi_i^0 = \|p_i\|^2/2$ then $\omega_i = 0$, where p_i is obtained using the formulae of the Section 4. In that case the Visibility diagram becomes a Voronoi diagram, hence $p_i \in \mathrm{V}_i(\psi^0)$.
- For the Point Source Mirror (PS/Mirror) case, an easy calculation shows that if we choose $\psi_i^0 = 1$, then $-y_i \in \mathrm{V}_i(\psi^0)$.
- For the Point Source Lens (PS/Lens) case, we can show that if we also choose $\psi_i^0 = 1$, then $y_i \in \mathrm{V}_i(\psi^0)$.

Remark that the previous expressions for ψ_0 ensure that $G_i(\psi^0) = \rho(V_i(\psi^0)) > 0$ only when the support X_ρ of the light source is large enough. As an example in the (PS/Mirror) case, if $-y_i \notin X_\rho$, then we may have $G_i(\psi^0) = 0$. To handle this difficulty, we use a linear interpolation between ρ and a constant function supported on a set that contains the $(-y_i)$'s. This is explained in more details in Section 6.3. This strategy also works for the (CS/Mirror), (PS/Lens) and (CS/Lens) cases.

5.3. **Damped Newton algorithm.** When the light source is collimated (*i.e.* $X = \mathbb{R}^2 \times \{0\}$), the problem is known to be an optimal transport problem in the plane for the quadratic cost, the function G is the gradient of a concave function, its derivative $\mathrm{D}G$ is symmetric and $\mathrm{D}G \leqslant 0$. Moreover, if $G_i(\psi) > 0$ for all i and if X_ρ is connected, then the kernel of $\mathrm{D}G$ is spanned by $\psi = \mathrm{cst}$. This ensures the convergence of the damped Newton algorithm [14] presented as Algorithm 2. Remark also that the matrix $\mathrm{D}G$ is very sparse, as the number of nonzero elements equals the number of edges in the graph induced by the visibility diagram. This also allows the use of efficient linear solvers in the Newton iterations. In this algorithm, A^+ denotes the *pseudo-inverse* of the matrix A.

When the light source is punctual (*i.e.* $X = \mathbb{S}^2$), we make the change of variable $\widetilde{\psi} = \ln(\psi)$ and $\widetilde{G} = G \circ \exp$, so that $G(\psi) = \sigma$ if and only if $\widetilde{G}(\tilde{\psi}) = \sigma$. This change of variable turns the optical component design problem into an optimal transport problem [7, 11], ensuring that $\widetilde{G}$ is the gradient of a concave function, and that $\mathrm{D}\widetilde{G}$ is symmetric non-positive. Note that in the (PS/Mirror) problem with convex mirrors, the damped Newton algorithm is also provably converging [14].

5.4. **Surface construction.** In the last step of Algorithm 1, we build a triangulation of the mirror or lens surface whose combinatorics is dual to the Visibility diagram. The input is a family of weights ψ solving Equation (LEC') and the parameterization function $\mathcal{R}_\psi$ whose formula is given in Section 3 and depends on the eight different cases. For each i, we compute $v_i = \mathcal{R}_\psi(c_i)$, where c_i is the centroid of the Visibility cell $V_i(\psi)$. The vertices of the triangulation are given by the v_i's and there is an edge between v_i and v_j if the Visibility cells $\mathrm{V}_i(\psi)$ and $\mathrm{V}_j(\psi)$ intersect. Examples of such triangulations can be found in Section 6. Remark that for each vertex v_i, we can compute exactly the normal to the (continuous surface) using Snell's law since we know the incident ray and the corresponding reflected or refracted direction y_i.

ALGORITHM 2: Damped Newton method for $G(\psi) = \sigma$

Input: A function $\rho : T \to \mathbb{R}^+$.
A function $\sigma = (\sigma_i)_{1 \leqslant i \leqslant N}$ supported on Y.
An initial vector ψ^0.
A tolerance $\eta > 0$.
Output: A vector ψ of $\mathbb{R}^N$.
Step 1: Transformation to an Optimal Transport problem
If $X = \mathbb{R}^2 \times \{0\}$**,:** then $\widetilde{\psi}^0 = \psi^0$ (and $\widetilde{G} = G$).
If $X = \mathbb{S}^2$**,:** then $\widetilde{\psi}^0 = (\ln(\psi_i^0))_{1 \leqslant i \leqslant N}$ (and $\widetilde{G} = (G_i \circ \exp)_{1 \leqslant i \leqslant N}$).
Step 2: Solve the equation: $\widetilde{G}(\widetilde{\psi}) = \sigma$
Initialization:
$\varepsilon_0 := \min\left[\min_i G_i(\psi^0),\ \min_i \sigma_i\right] > 0$.
$k = 0$.
While: $\left\|\widetilde{G}(\widetilde{\psi}^k) - \sigma\right\|_\infty \geqslant \eta$
-: Compute $d_k = -\mathrm{D}\widetilde{G}(\widetilde{\psi}^k)^+(\widetilde{G}(\widetilde{\psi}^k) - \sigma)$
-: Determine the minimum $\ell \in \mathbb{N}$ such that $\widetilde{\psi}^{k,\ell} := \widetilde{\psi}^k + 2^{-\ell} d_k$ satisfies

$$\begin{cases} \min_i \widetilde{G}_i(\widetilde{\psi}^{k,\ell})) \geqslant \varepsilon_0 \\ \left\|\widetilde{G}(\psi^{k,\ell}) - \sigma\right\|_\infty \leqslant (1 - 2^{-(\ell+1)}) \left\|\widetilde{G}(\widetilde{\psi}^k) - \sigma\right\|_\infty \end{cases}$$

-: Set $\widetilde{\psi}^{k+1} = \widetilde{\psi}^k + 2^{-\ell} d_k$ and $k \leftarrow k + 1$.
Return: $\psi := (\widetilde{\psi}_i^k)_{1 \leqslant i \leqslant N}$ if $X = \mathbb{R}^2 \times \{0\}$ or
$\psi := (\exp(\widetilde{\psi}_i^k))_{1 \leqslant i \leqslant N}$ if $X = \mathbb{S}^2$.

6. Results and Discussion

In this section, we present several numerical examples for the different problems previously described as well as some other applications.

In the experiments, we take $\kappa = 1.5$ for the collimated light source lenses and $\kappa = 2/3$ for the point light source lenses. Unless said otherwise, the light source is chosen to be uniform and the discretization of the target (number of Diracs N) is chosen to be equal to the size of the image.

6.1. **Evaluation.**

6.1.1. *Numerical evaluation.* Let us recall that our algorithm takes as a parameter the numerical error η. This means that using Algorithm 1, one can solve any of the eight optical component design problems previously described as precisely as wanted.

6.1.2. *Qualitative evaluation through rendering.* We choose to use two different rendering methods: a simple one using a basic raytracing algorithm and another one using the physically based renderer *LuxRender*.

- **Raytracing:** The light source is simulated by randomly choosing points either on a 2D domain (collimated source) or on the unit sphere (point source), then computing the reflected (or refracted) ray emanating from this point. Each hit on the screen increments the intensity of the corresponding pixel. Note that the normal at the hit point on the surface is computed using a $\mathcal{C}^1$ interpolation scheme known as Clough-Tocher scheme [1].

- **LuxRender:** For more complex scenes, such as the ones in Figure 1, we use the LuxRender rendering engine (with the Stochastic Progressive Photon Mapping rendering method combined with a traditional Metropolis sampler).

Let us remark that even though both of these renderings are physically realist, the first one is more accurate: LuxRender is simulating the trajectory of the light reflected or refracted by a triangulation which is an approximation of an optical component $\mathcal{R}$. Our first raytracing is also simulating the trajectory of the light, but is using an approximation of the surface with more accurate normals, since the Clough-Tocher scheme creates a C^1 surface that interpolates the normal of the optical component $\mathcal{R}$.

6.2. **Results.**

6.2.1. *Genericity.* Our algorithm is able to solve eight different optical component design problems. We present for instance in Figure 4 four examples for which we display the Visibility diagram of X_ρ as well as the optical component (lens or mirror) above it, a mesh of the optical component and a forward simulation using raytracing.

Then, for the examples of Figures 5, 6, 8 and 9, we display the target distribution as an image; a mean curvature plot (blue represents low mean curvature and red high mean curvature) of the constructed mesh $\mathcal{R}_T$ and a forward simulation using raytracing.

6.2.2. *High-contrast and complex target lights.* We can handle any kind of target light. Figures 5 and 6 shows several examples of mirror design for respectively a collimated and a point light source. Note that we are able to construct mirrors for smooth images such as the Cameraman (first row) or Lena (second row) images as well as images with totally black areas (third and fourth rows). We are also able to handle target supported on *non-convex* sets such as the Hikari and Siggraph images. One can notice that since the area of the Visibility cells are equal to the greyscale values of the image then the triangles have roughly the same size, implying that one can recognize the target image in the mesh of the surface, see Figure 7 for zooms on different meshes. The mean curvature plot shows the discontinuities in the surface which come from the black areas in the image. Figures 8 and 9 show the same kind of results for the lens design problems (CS/Lens) and (PS/Lens).

Figure 10 shows results with increasing discretizations of the same target for the (PS/Mirror) and (CS/Lens) problems. One can remark that if we subsample the image (second column) then the forward simulation is pixelated as expected. On the contrary, if we oversample (fourth column), then the rendered image is smoother but is blurred.

6.2.3. *Convex / concave optical components.* As shown in Section 3, for each problem, one can choose between two different parameterizations. For instance, for the (CS/Lens) problem, one can build a lens which is either concave or convex, see Figure 11 for an illustration of these differences. Furthermore, one can notice that when the optical component is not convex nor concave, the quality of the forward simulation is less accurate, as illustrated in the last row of Figures 4 and in Figure 9. We suspect that the triangulation $\mathcal{R}_T$ of the lens surface $\mathcal{R}$ is not a sufficiently good approximation when there is a lack of regularity. We emphasize that we choose not

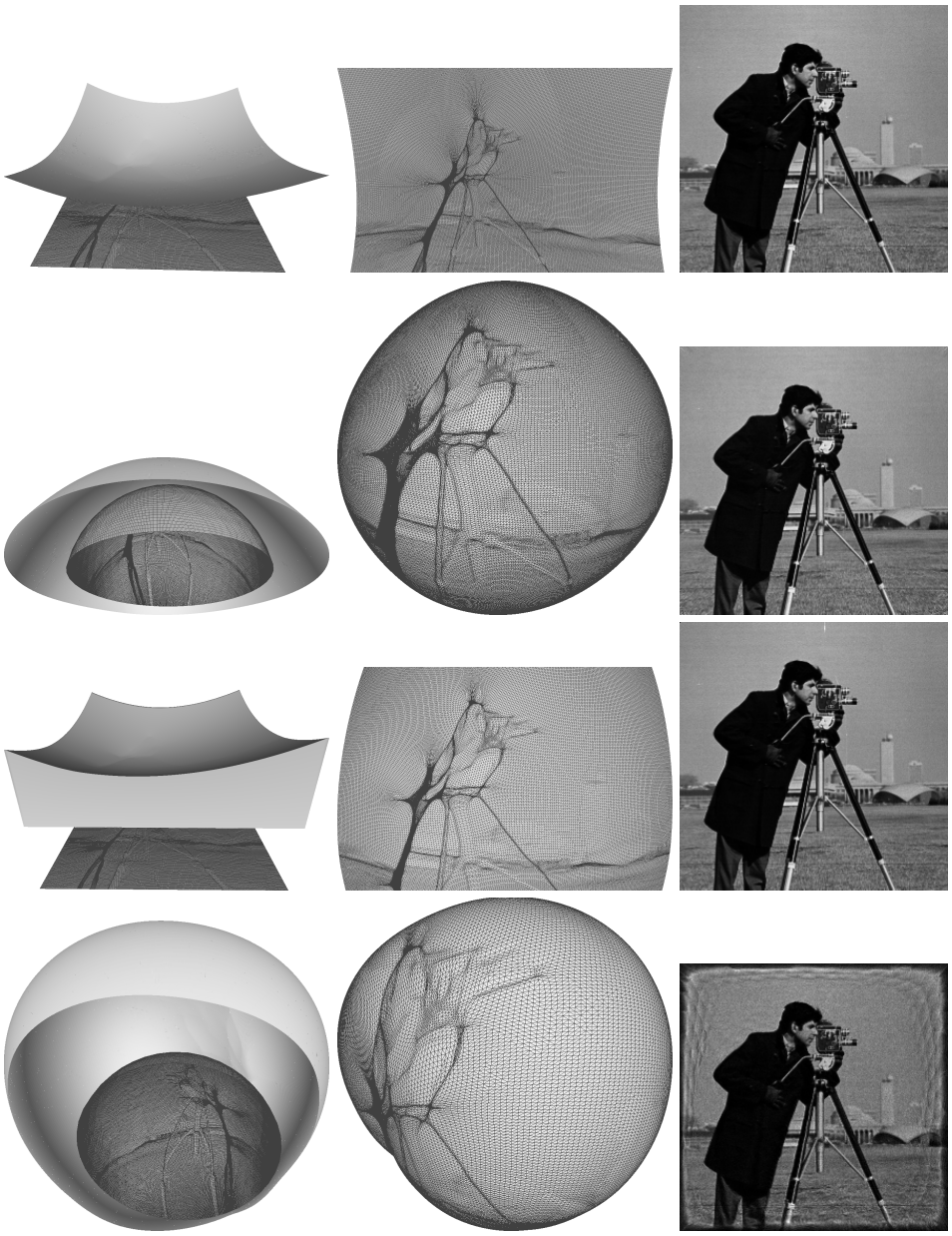

FIGURE 4. **Four non-imaging problems solved with Algorithm 1**. *From left to right:* Visibility diagram on X_ρ (wireframe) with the optical component $\mathcal{R}$, Triangulation $\mathcal{R}_T$ of $\mathcal{R}$; forward simulation with raytracing (10^7 rays). *From top to bottom:* Convex Collimated Source Mirror; Concave Point Source Mirror; Concave Collimated Source Lens; Point Source Lens (with the union of ellipsoids).

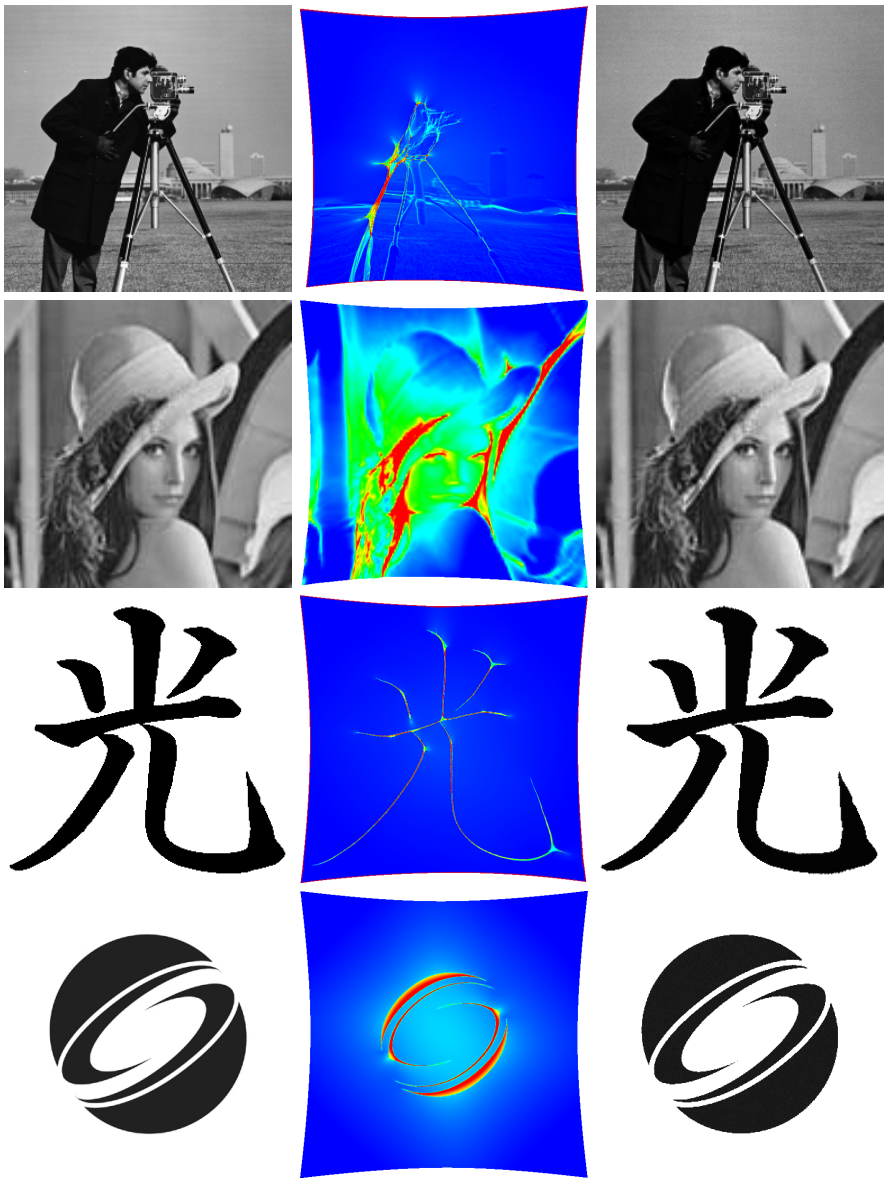

FIGURE 5. **Convex Collimated Source Mirror** problem with a uniform light source for different target distributions. *From left to right:* target distribution, mean curvature plot of the mirror, forward simulation (10^8 rays). Dimensions of the images from top to bottom: 256x256, 128x128, 300x300, 400x400.

to improve the quality of the forward simulation by post-processing $\mathcal{R}_T$, in order to show the need of designing optical components with nice geometric properties.

6.2.4. *Non-uniform light sources.* We we can also use our algorithm with non-uniform light sources. Figure 12 shows an example where the source is chosen

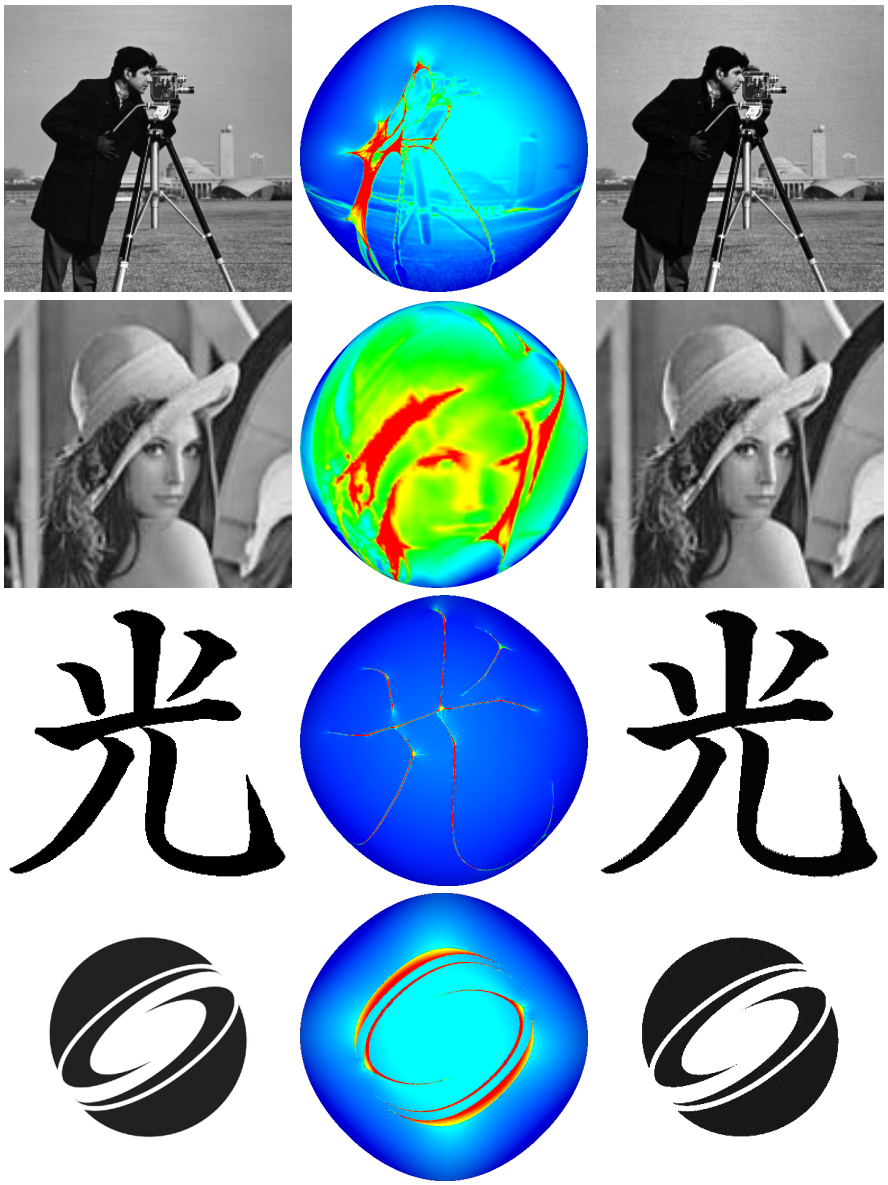

FIGURE 6. **Concave Point Source Mirror** problem for a uniform point light source with different target distributions. *From left to right:* target distribution, mean curvature plot of the mirror (top view), forward simulation (10^8 rays). Dimensions of the images from top to bottom: 256x256, 128x128, 300x300, 400x400.

to be a Gaussian for the (CS/Lens) case. One can notice that due to the concentration of the light, the details of the triangulation are more concentrated in the middle.

6.2.5. *Comparison with previous work.* Figure 13 compares the renderings obtained by our method (second column) and the state of the art results presented in [22] (third column) on two target distributions for the (CS/Lens) case with a collimated uniform light source. One can notice, in the second column, the presence of small artifacts between the black and white regions, for instance around the rings (notably in the center). The contrast is also more accurate with our convex lenses.

6.2.6. *Performance.* The algorithm takes 1687 seconds and 13 iterations in the Newton algorithm to solve the (CS/Mirror) case for the CAMERAMAN target. We underline that the number of iterations in the Newton step remains low: in all our examples it varies from 10 to 20. This means that the computational cost of the method is concentrated in the computation of the functional G, its derivative $\mathrm{D}G$ and the resolution of the linear system. We believe that there is much room for improvement in the first two steps, by optimizing the computation of Visibility cells, and by using an explicit computation of $\mathrm{D}G$ instead of relying on automatic differentiation.

6.3. **Application to pillows.** The problem consists in decomposing the optical component (mirror or lens) into several small optical components that are called *pillows*, as illustrated in Figure 1. Each pillow independently satisfies the same non-imaging problem with the same target light. Hence, the optical component made with all the small pillows glued together is more reliable and allows for example to reduce artifacts due to small occluders. Indeed if one object is in front of one or more lenses, the quality of the refracted image decreases but the image can still be recognized. This has applications for instance in car headlight design [2].

The main difficulty in the design of each pillow is the choice of the initial weights ψ^0. Indeed, the choices detailed in Section 5.2 only work when the support of the source intensity function is large enough. To solve this problem using our current approach, we linearly interpolate between a constant density defined on the support X_ρ of the light source intensity function ρ and the restriction of ρ to the localization $X_\rho^\ell \subset X_\rho$ of the pillow. In practice, X_ρ is the whole hemisphere or a large portion of the plane $\mathbb{R}^2 \times \{0\}$, a geometric setting for which we know how to choose the initial weights.

In practice, we partition the support X_ρ of the optical component into several patches $X_\rho = \cup_\ell X_\rho^\ell$. We then solve the mirror or lens problem for each pillow $\mathcal{R}^\ell$ parameterized over the set X_ρ^ℓ with Algorithm 3. We can show that Step 2 of this algorithm allows to find a family of weights ψ for which we have the required condition $G_i(\psi) > 0$ for each $i \in \{1, \cdots, N\}$. Indeed, a straightforward calculation shows that when we choose $\epsilon_0 < \min_i \sigma_i - \eta$, then the Visibility cells associated to $\psi = \texttt{DAMPED\_NEWTON}(T, \rho_\epsilon^\ell, Y, \sigma, \psi, \eta)$ have to intersect X_ρ^ℓ, hence their integrals $G_i(\psi)$ do not vanish. We then have a collection of triangulations $\mathcal{R}_T^\ell$. A global mirror (or lens) can then be constructed using the fact that each $\mathcal{R}_T^\ell$ is a graph above X_ρ^ℓ. An example with 9 pillows can be found in Figure 1. One can notice the shadow on the screen due to the occlusion of some lenses by the red obstacle.

In practice, in order to avoid a shift between the nine simulated images in Figure 1, we target points in the plane at finite distance (instead of the unit sphere) containing the desired image and use our algorithm iteratively on the projection of these points onto the unit target sphere.

6.4. **Limitations.** The main limitation of our approach is the fact that we only deal with ideal light sources. If we replace for instance the collimated light with a real light like the sun, since there will be more than one incident ray for a given surface point, thus resulting in a slightly blurred rendering.

Furthermore, the Automatic Differentiation technique used in Section 5 is useful to have a generic algorithm but adds an important computational overhead to the code.

ALGORITHM 3: Mirror / lens construction (for a pillow $\mathcal{R}^\ell$)

Input: A function $\rho^\ell_{in} : X_\rho \to \mathbb{R}^+$ with support $X^\ell_\rho \subset X_\rho$.
A target light intensity function σ_{in}.
A tolerance $\eta > 0$.
Output: A triangulation $\mathcal{R}^\ell_T$ of a mirror or lens $\mathcal{R}^\ell$.
Step 1: Initialization
$T, \rho^\ell \leftarrow$ `DISCRETIZATION_SOURCE`(ρ^ℓ_{in})
$Y, \sigma \leftarrow$ `DISCRETIZATION_TARGET`(σ_{in})
$\psi^0 \leftarrow$ `INITIAL_WEIGHTS`(Y) (Section 5.2)
Set $\epsilon = 1$, $\psi = \psi^0$ and $\epsilon_0 = (\min_i \sigma_i - \eta)/2$.
Step 2: Find initial weights ψ, s.t. $V_i(\psi) \cap X^\ell_\rho \neq \emptyset \ \forall i \in \{1, \cdots, N\}$
While: $\epsilon > \epsilon_0$
$\rho^\ell_\epsilon \leftarrow \epsilon \mathbf{1}_{X_\rho} + (1-\epsilon)\rho^\ell$. ($\mathbf{1}_{X_\rho}$ is the indicator function of X_ρ)
$\psi \leftarrow$ `DAMPED_NEWTON`$(T, \rho^\ell_\epsilon, Y, \sigma, \psi, \eta)$
$\epsilon \leftarrow \epsilon/2$
Step 3: Solve (LEC') on X^ℓ_ρ
Return $\psi :=$ `DAMPED_NEWTON`$(T, \rho^\ell, Y, \sigma, \psi, \eta)$
Step 4: Construct a triangulation $\mathcal{R}^\ell_T$ of $\mathcal{R}^\ell$
$\mathcal{R}^\ell_T \leftarrow$ `SURFACE_CONSTRUCTION`$(\psi, \mathcal{R}_\psi)$

7. Conclusion and perspectives

We presented a robust and parameter-free method able to solve eight different optical component design problems satisfying light energy constraints. We proposed an efficient algorithm able to solve them. The approach is based on the structure of the Visibility diagram associated to a problem and its relation to a restricted 3D Power diagram. It seems likely that the same approach can be applied to other optical component design problems such as having a target at fixed distance (near field target). We also believe that the robustness and versatility of the proposed approach can make it a useful component for the design of heuristics able to deal with extended light sources.

References

1. Peter Alfeld, *A trivariate clough-tocher scheme for tetrahedral data*, Computer Aided Geometric Design **1** (1984), no. 2, 169–181.
2. Julien André, Dominique Attali, Quentin Mérigot, and Boris Thibert, *Far-field reflector problem under design constraints*, International Journal of Computational Geometry & Applications **25** (2015), no. 02, 143–162.
3. L Caffarelli, S. Kochengin, and VI Oliker, *On the numerical solution of the problem of reflector design with given far-field scattering data*, Contemporary Mathematics **226** (1999), 13–32.
4. L. A. Caffarelli and V. Oliker, *Weak solutions of one inverse problem in geometric optics*, Journal of Mathematical Sciences **154** (2008), no. 1, 39–49.

5. Luis A Caffarelli, Cristian E Gutiérrez, and Qingbo Huang, *On the regularity of reflector antennas*, Annals of mathematics **167** (2008), no. 1, 299–323.
6. F. Cork, D.F. Bettridge, and P.C. Clarke, *Method of and mixture for aluminizing a metal surface*, February 22 1977, US Patent 4,009,146.
7. Pedro Machado Manhães de Castro, Quentin Mérigot, and Boris Thibert, *Far-field reflector problem and intersection of paraboloids*, Numerische Mathematik (2015), 1–23.
8. Fernando de Goes, Katherine Breeden, Victor Ostromoukhov, and Mathieu Desbrun, *Blue noise through optimal transport*, ACM Transactions on Graphics **31** (2012), no. 6, 171.
9. Manuel Finckh, Holger Dammertz, and Hendrik PA Lensch, *Geometry construction from caustic images*, Computer Vision–ECCV 2010, Springer, 2010, pp. 464–477.
10. T Glimm and V Oliker, *Optical design of single reflector systems and the monge–kantorovich mass transfer problem*, Journal of Mathematical Sciences **117** (2003), no. 3, 4096–4108.
11. Cristian E Gutiérrez and Qingbo Huang, *The refractor problem in reshaping light beams*, Archive for rational mechanics and analysis **193** (2009), no. 2, 423–443.
12. Cristian E Gutiérrez and Federico Tournier, *The parallel refractor*, From Fourier Analysis and Number Theory to Radon Transforms and Geometry, Springer, 2013, pp. 325–334.
13. Thomas Kiser, Michael Eigensatz, Minh Man Nguyen, Philippe Bompas, and Mark Pauly, *Architectural caustics–controlling light with geometry*, Citeseer, 2012.
14. Jun Kitagawa, Quentin Mérigot, and Boris Thibert, *A newton algorithm for semi-discrete optimal transport*, arXiv preprint arXiv:1603.05579 (2016).
15. Bruno Lévy, *A numerical algorithm for l^2 semi-discrete optimal transport in 3d*, arXiv preprint arXiv:1409.1279 (2014).
16. Q. Mérigot, *A multiscale approach to optimal transport*, Computer Graphics Forum, vol. 30, Wiley Online Library, 2011, pp. 1583–1592.
17. Jean-Marie Mirebeau, *Discretization of the 3d monge-ampere operator, between wide stencils and power diagrams*, arXiv preprint arXiv:1503.00947 (2015).
18. Marios Papas, Wojciech Jarosz, Wenzel Jakob, Szymon Rusinkiewicz, Wojciech Matusik, and Tim Weyrich, *Goal-based caustics*, Computer Graphics Forum, vol. 30, Wiley Online Library, 2011, pp. 503–511.
19. Gustavo Patow and Xavier Pueyo, *A survey of inverse surface design from light transport behavior specification*, Computer Graphics Forum, vol. 24, Wiley Online Library, 2005, pp. 773–789.
20. CR Prins, Thije Boonkkamp, van J Jarno Roosmalen, WL IJzerman, and TW Tukker, *A numerical method for the design of free-form reflectors for lighting applications*, Technische Universiteit Eindhoven, 2013.
21. Louis B Rall, *Automatic differentiation: Techniques and applications*, (1981).
22. Yuliy Schwartzburg, Romain Testuz, Andrea Tagliasacchi, and Mark Pauly, *High-contrast computational caustic design*, ACM Transactions on Graphics (TOG) **33** (2014), no. 4, 74.
23. X.J. Wang, *On the design of a reflector antenna ii*, Calculus of Variations and Partial Differential Equations **20** (2004), no. 3, 329–341.
24. Tim Weyrich, Pieter Peers, Wojciech Matusik, and Szymon Rusinkiewicz, *Fabricating microgeometry for custom surface reflectance*, ACM Transactions on Graphics (TOG) **28** (2009), no. 3, 32.
25. Yonghao Yue, Kei Iwasaki, Bing-Yu Chen, Yoshinori Dobashi, and Tomoyuki Nishita, *Pixel art with refracted light by rearrangeable sticks*, Computer Graphics Forum, vol. 31, Wiley Online Library, 2012, pp. 575–582.
26. ———, *Poisson-based continuous surface generation for goal-based caustics*, ACM Transactions on Graphics (TOG) **33** (2014), no. 3, 31.

Laboratoire de mathématiques d'Orsay, Université Paris-Sud, Orsay, France

GIPSA-Lab, Grenoble INP, Grenoble, France & Laboratoire Jean Kuntzmann, Université Grenoble-Alpes, Grenoble, France

Laboratoire Jean Kuntzmann, Université Grenoble-Alpes, Grenoble, France

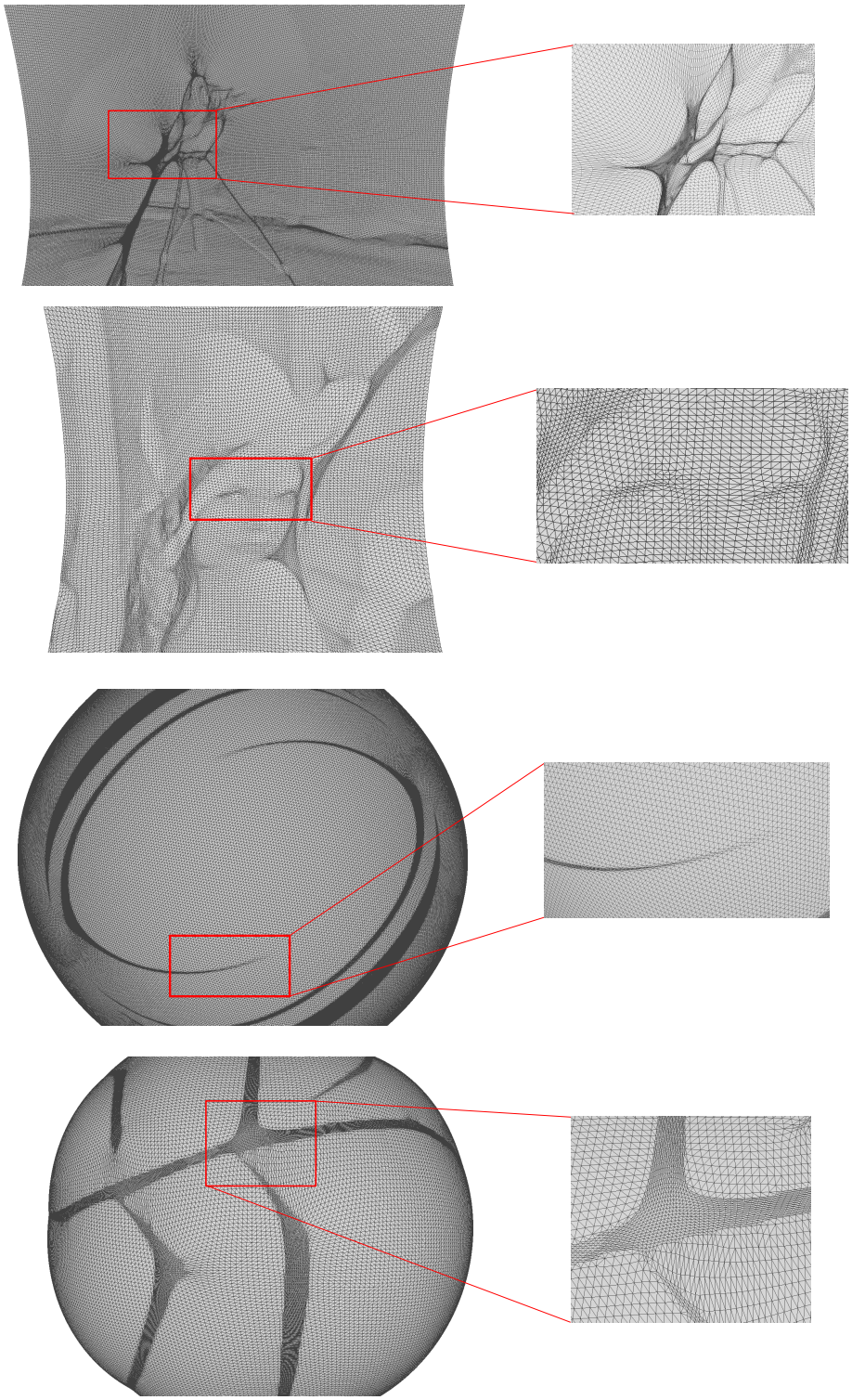

FIGURE 7. **Triangulations $\mathcal{R}_T$ of several optical components** seen from above. *From top to bottom:* Convex Collimated Source Mirror, Concave Collimated Source Lens, Concave Point Source Mirror and Point Source Lens.

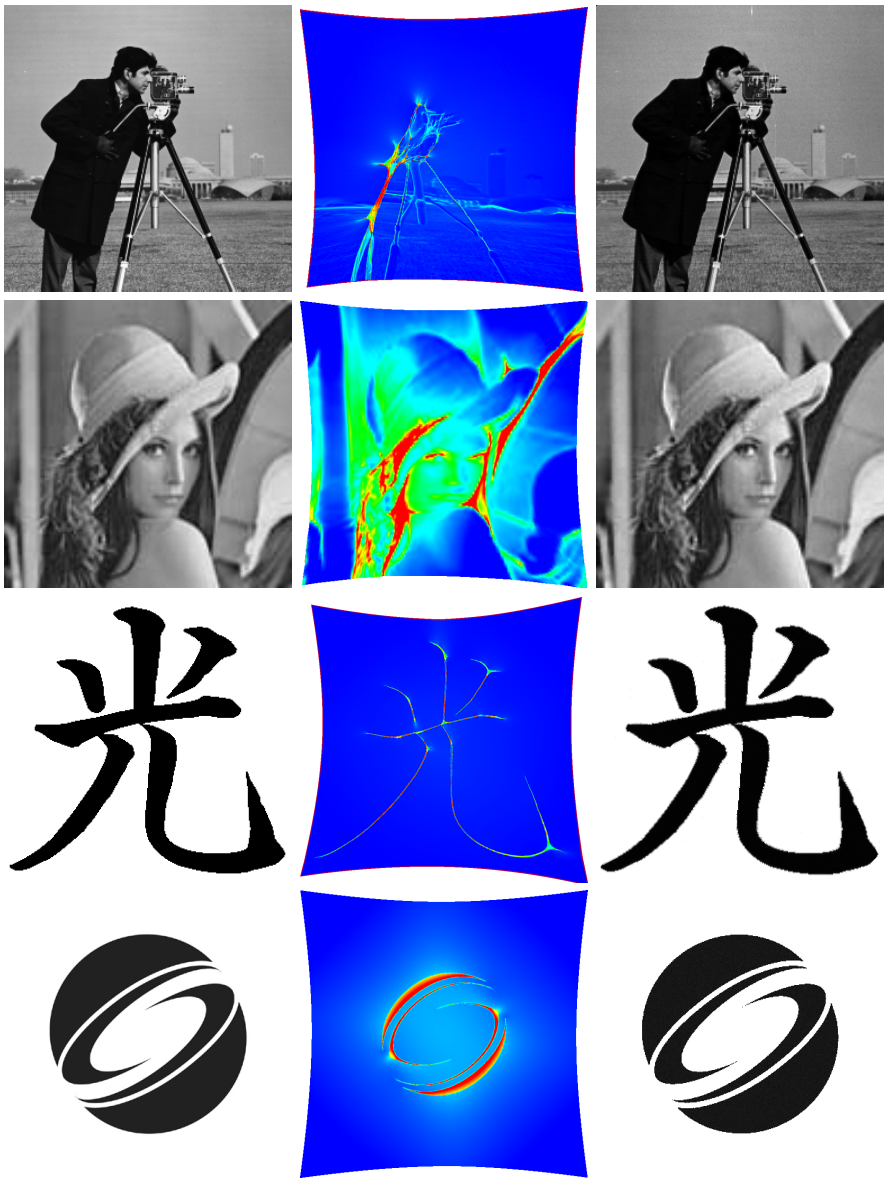

FIGURE 8. **Concave Collimated Source Lens** with a uniform light source for different target distributions. *From left to right:* target distribution, mean curvature plot of the lens (top view), forward simulation (10^8 rays). Dimensions of the images from top to bottom: 256x256, 128x128, 300x300, 400x400.

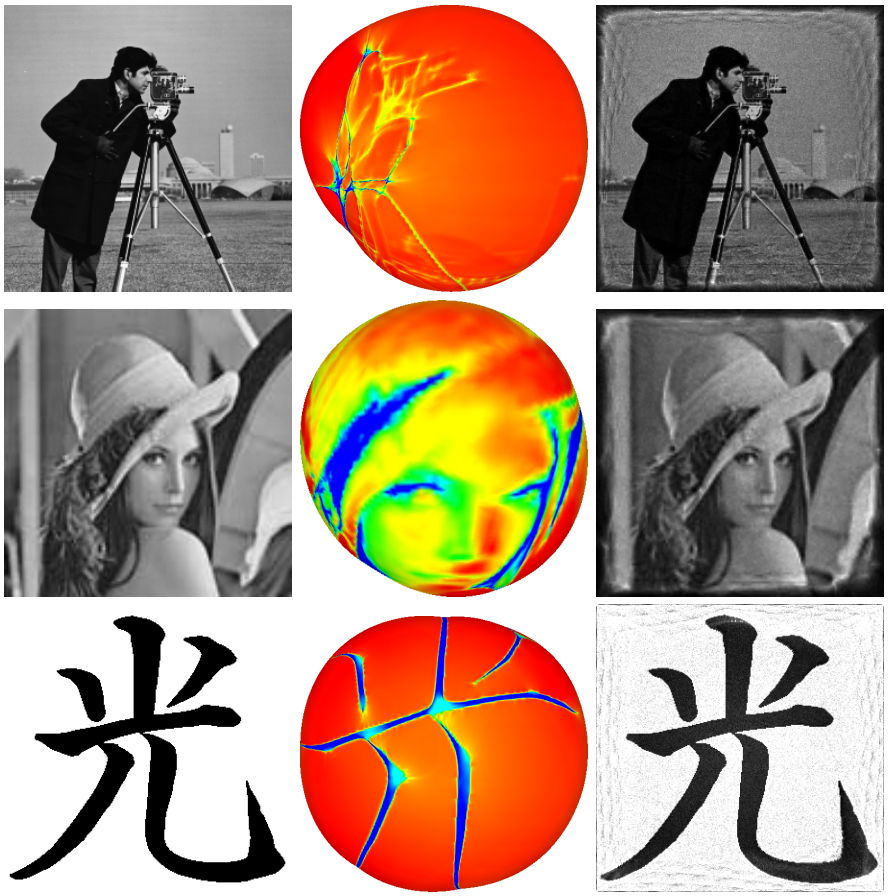

FIGURE 9. **Point Source Lens** with a uniform light source for different target distributions. The lens surface is the boundary of the union of filled ellipsoids, hence is not convex, nor concave. *From left to right:* target distribution, mean curvature plot of the lens (top view), forward simulation (10^7 rays). Dimensions of the images from top to bottom: 256x256, 128x128, 300x300.

FIGURE 10. **Comparison for different discretizations.** Comparison of the forward simulations for the Point Source Mirror (first row) and Collimated Source Lens (second row) problems with different discretizations of the same target distribution. The dimensions of the original image (left) are 128x128. Then from left to right, the discretizations are the following: 64x64, 128x128, 256x256.

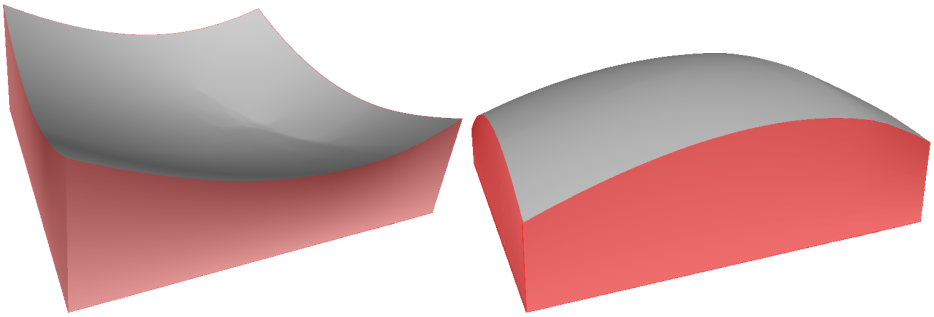

FIGURE 11. **Concave and convex lenses** for a uniform collimated light source and the cameraman target.

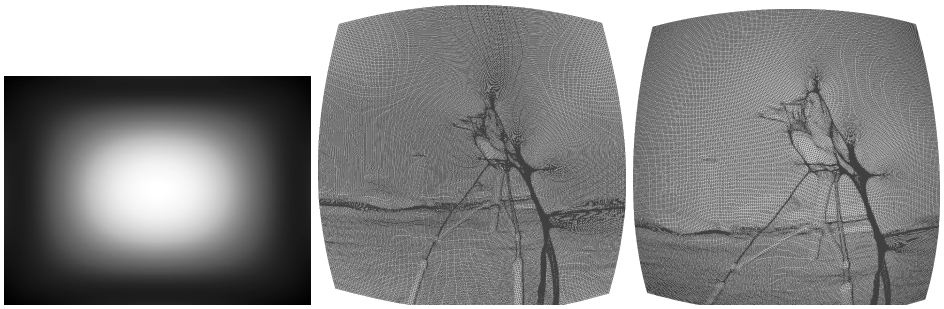

FIGURE 12. **Triangulation $\mathcal{R}_T$ for a non-uniform light source.** *From left to right*: non uniform collimated light source; mesh of the lens for this non-uniform light; mesh of the lens for a uniform light source.

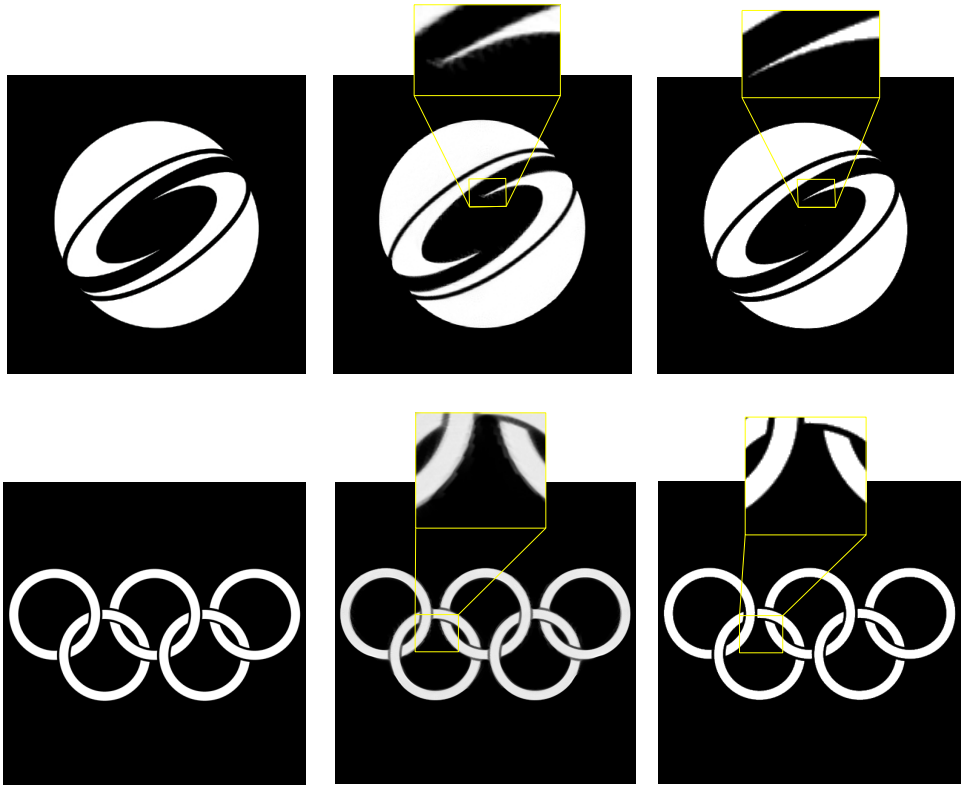

FIGURE 13. **Comparison with** [22] *From left to right:* target distribution; images obtained by [22] and taken from their article; our forward simulation using raytracing (10^8 rays).